Progress In Electromagnetics Research C, Vol. 69, 139–146, 2016

Compact UHF RFID Handheld Reader Antenna and Array Based on Resonant Quadrifilar Spiral Structure

Xuefeng Zhao[1, 2], Yongjun Huang[1, *], Jian Li[1], Qing Zhang[1], and Guangjun Wen[1]

Abstract—In this paper, a compact circularly polarized antenna based on a resonant quadrifilar spiral structure for the application of UHF RFID handheld reader is proposed and demonstrated experimentally. To reduce antenna size and improve impedance matching, the original resonant arms are revised by bending inverted-F structures and printing them on dielectric substrates, and the four arms are fed by a four-way phase shift network. Such an antenna indicates stable circular polarization performance and wide beamwidth. The gain bandwidth (> 2 dBic) can cover the frequency band from 902 MHz to 928 MHz, which is suitable for most of the popular UHF RFID systems in the world. Moreover, the 1×4 array and 2×2 array based on previously demonstrated antenna unit are numerically investigated. The array performances, including the gain, beam scanning and low side-lobe are discussed.

1. INTRODUCTION

Radio frequency identification (RFID), as an emerging technology for contactless automatic identification, is widely used in retail, transportation logistics, warehouse management, access control, etc., in recent years [1, 2]. Ultra-high-frequency (UHF) RFID means that the RFID technique operates within 840–960 MHz frequency band. Since UHF RFID has many exciting merits, such as fast reading rate, long writing distance, multi-target recognition and fast-moving target identification, this technique has received considerable research attention by government and industry, which makes UHF RFID developed rapidly. Reader antenna, as a key component of RFID system, will directly affect the performance of the whole RFID system. Reader antenna is usually required to be circularly polarized [3]. According to some applications, reader antenna is also required to have wide band, be miniaturized, and in low cost [4–6]. Moreover, a phased array antenna has a high gain and can realize beam scanning quickly and flexibly. Therefore, phased array antenna technology is usually applied to the UHF RFID systems, in order to extend reader's coverage range and improve reading rate [7–9].

Specifically, the compact circularly polarized antenna for the application of UHF RFID handheld reader has recently been developed quickly [10–20]. Those antennas are realized by using asymmetric-circular shaped slotted microstrip, cross-shaped slotted microstrip [10, 11, 13], crossed dipoles with different shapes [14–16], four meandered monopoles [17], X-shaped slotted square-patch with cross-strip proximity-fed technique [18], and Koch fractal geometry [20]. Most of those designs realize circular polarization by integrating a four-way phase shift network. Moreover, researchers proposed a type of printed square quadrifilar spiral antenna for the UHF RFID handheld reader applications [21, 22]; however, the performance is not good enough. Quite recently, researchers have developed an universal UHF RFID handheld reader antenna with rotated inverted-F antennas [23], while the antenna size is not compact enough.

Received 10 October 2016, Accepted 3 November 2016, Scheduled 21 November 2016

* Corresponding author: Yongjun Huang (yongjunh@uestc.edu.cn).

[1] Centre for RFIC and System Technology, School of Communication and Information Engineering, University of Electronic Science and Technology of China, Chengdu 611731, China. [2] School of Computer Engineering, Huaihai Institute of Technology, Lianyungang 222005, China.

In this paper, a compact, low-cost, wideband circularly polarized UHF RFID hand-held reader antenna is presented and analyzed. To reduce antenna size and improve impedance matching bandwidth, the original resonant arms are revised by bending inverted-F structures and printing them on dielectric substrates. The four arms are fed by a compact four-way phase shift network. Such an antenna indicates stable circular polarization performance and wide beamwidth. The gain bandwidth (> 2 dBic) can cover the frequency band from 902 MHz to 928 MHz, which is suitable for most of the popular UHF RFID systems in the world. Moreover, the 1×4 array and 2×2 array based on previously demonstrated antenna unit are numerically investigated. The array performances, including the gain, beam scanning and low side-lobe are discussed, and the results indicate that the arrays are useful for the phased array applications in RFID fields.

2. ANTENNA UNIT DESIGN AND NUMERICAL SIMULATIONS

The proposed antenna unit based on a resonant quadrifilar spiral structure with a four-way phase shift network is shown in Fig. 1(a). For the top layer, four quadrifilar spirals are printed on a 0.508 mm dielectric substrate (relative permittivity $\epsilon_r = 3.9$, loss tangent $\tan\delta = 0.008$) and then are connected to inverted-F structures accordingly with metallic vias. The four inverted-F structures are printed on another two cross dielectric layers, and then the input ports of such four inverted-F structures are fed by a four-way phase shift network. The design details for the quadrifilar spirals, four-way phase shift network, and inverted-F structures can be found in Figs. 1(b)–(d).

The designed antenna is developed from a classic quadrifilar spiral structure [24] with $1/4\lambda$ spiral length. Therefore, it can exhibit circular polarization once the four spirals are fed by equal magnitude and ± 90 deg phase delay. However, the impedance of the four spirals is smaller than 10 ohm, which makes it difficult to match directly to the regular 50 ohm connectors. The four integrated inverted-F structures are used to enhance the impedance of the spiral and at the same time reduce the antenna size. The circular polarization (left hand or right hand) can be achieved by feeding the four spirals with increased or decreased 90 deg phased difference. In this paper, as an example, the left-handed circularly polarized (LHCP) antenna is discussed, and the phase difference can be obtained in Figs. 1(b) and (c). To achieve high performance circular polarization for the proposed antenna, the four-way phase shift network is critical, and the meandered configuration is shown in Fig. 1(c). The microstrip linewidth and length of the phase shift network are determined firstly with LineCal Kit of ADS software, to achieve the specific impedance and phase delay requirements. As shown in the right-upper part in Fig. 1(c), due to the overlapping of two microstrip lines, one of the lines is connected with two vias.

The performance of the four-way phase shift network is then optimized with HFSS software, based on the previous obtained parameters. In HFSS optimization, the input port connecting to the 50 ohm SMA cable is defined as Port 5. The port impedance of other four ports is 100 ohm. The finally optimized reflection curve for Port 5 (input port) is shown in Fig. 2(a) with optimized parameters: $w_1 = w_3 = 1.02$ mm, $w_2 = 0.53$ mm, and $w_4 = 0.22$ mm. The magnitude and phase of the four output ports are concluded in Figs. 2(b) and (c) accordingly. As can be seen in Fig. 2, the proposed network is

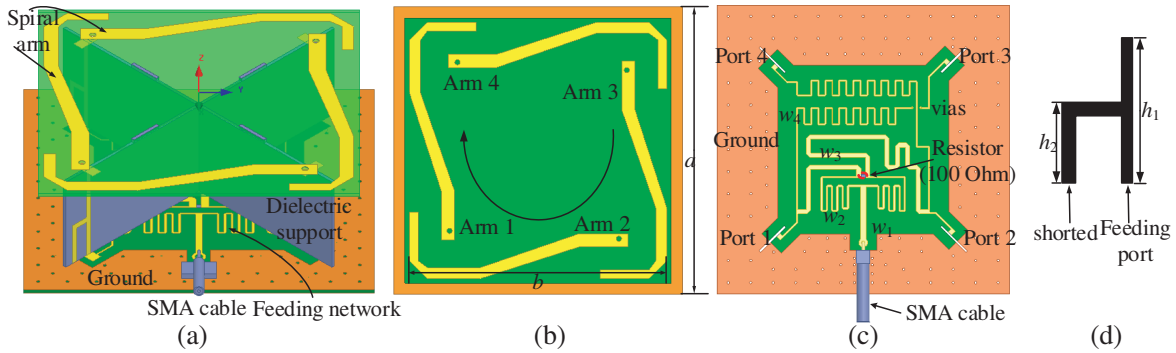

Figure 1. (a) The schematic representation for the proposed antenna, (b) top layer with four quadrifilar spirals, (c) bottom layer with the four-way phase shift network, and (d) the definition of the inverted-F structures.

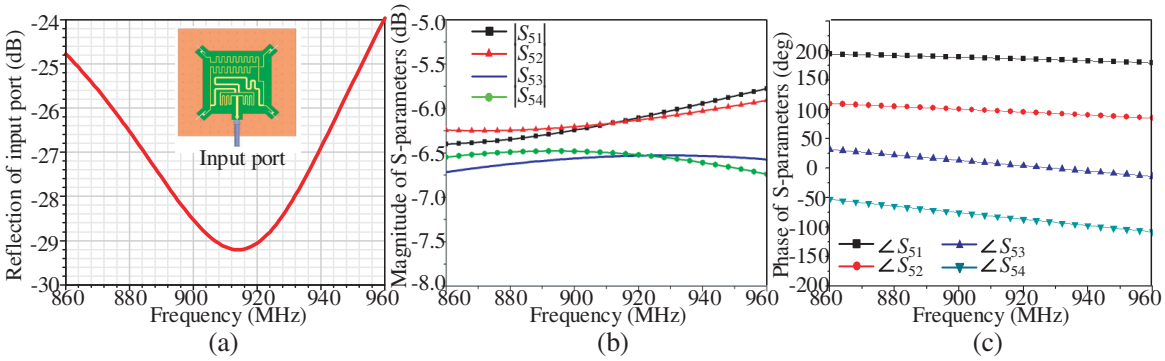

Figure 2. Optimized (a) reflection of input port, (b) magnitude and (c) phase performance of the four output ports.

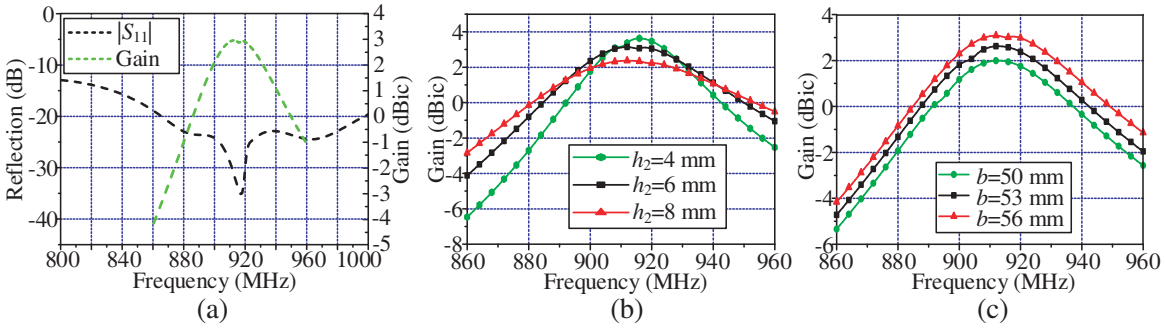

Figure 3. (a) Optimized reflection and far-field radiation gain performance of the proposed antenna, and the gain changing properties with different (b) h_2 and (c) b.

impedance matched well to 50 ohm for the input port. The powers at four output ports are almost the same with minor difference within 0.5 dB, and the phase delay for the four output ports satisfies 90 deg difference sequently, in the whole UHF frequency band. It means that the designed four-way phase shift network can be used to feed the quadrifilar spirals to achieve high performance circular polarizations.

Then the whole antenna as shown in Fig. 1(a) is co-simulated and optimized. The optimized reflection of the proposed antenna is shown in Fig. 3(a) (black dashed line) and the optimized main structural parameters are: $a = 60$ mm, $b = 56$ mm, $h_1 = 9$ mm, and $h_2 = 6$ mm. The length of the four quadrifilar spirals are determined as 1/4 wavelength corresponding to the center frequency, e.g., 915 MHz. It can be seen from Fig. 3(a) that the proposed antenna has a very wide impedance bandwidth ($|S_{11}| < 10$ dB) covering all the simulated frequency band. The obtained far-field radiation gain as shown in Fig. 3(a) (green dashed line) indicates that the proposed antenna has a peak gain about 3.1 dBic, which drops quickly when the frequency offsets from the center frequency.

Because the proposed antenna has a very wide impedance bandwidth compared to the gain bandwidth, here we mainly discuss the effects of some key structural parameters on the gain performances. As shown in Fig. 3(b), when changing parameter h_2 from 4 mm to 8 mm, the radiation gain curves are changed. Specifically, the peak gain is reduced and the gain bandwidth increased with increased h_2. Therefore, we choose the value of 6 mm as h_2 in the final structure to get moderate peak gain and gain bandwidth. As shown in Fig. 3(c), when increasing the parameter b from 50 mm to 56 mm, the gain in the whole simulated frequency band is increased. This is mainly due to the reduction of coupling among the four arms when the distances among those arms are increased. So in the limited space, we choose the maximum value to get the best radiation gain performance.

The simulated far-field radiation patterns at x-z plane and y-z plane at 915 MHz for the LHCP antenna proposed in this paper are shown in Figs. 4(a) and (b), which show quite good circular polarization performances for both main planes. Moreover, the simulated axial ratio versus vertical angle as shown in Fig. 4(c) indicates that the optimized antenna has a 3-dB axial ratio beamwidth about 120 deg for both main planes.

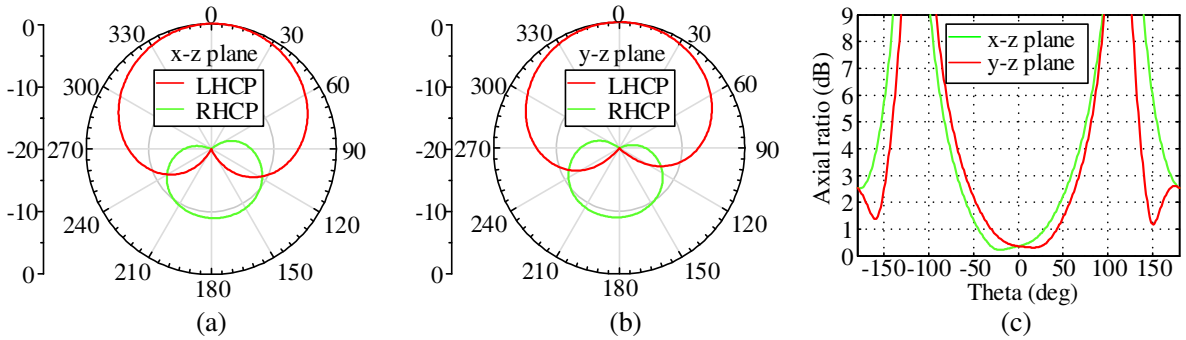

Figure 4. The simulated far-field radiation pattern (normalized) at (a) x-z plane and (b) y-z plane, and (c) axial ratio performance at both main planes, for the proposed antenna.

3. ANTENNA UNIT DEMONSTRATIONS

Based on the obtained structural parameters in previous section, here we fabricate this antenna, and the assembled prototype can be found in the inset of Fig. 5(a). The port reflection is firstly measured by a vector network analyzer (Agilent N5230A), and the result is shown in Fig. 5(a). The corresponding simulated curve is copied here for comparison. It can be seen that a good agreement between simulation and measurement is obtained, especially the resonance and changing feature. The measured reflection is below -10 dB in the whole measured frequency band. The far-field radiation gain and axial ratio in the frequency range (860 MHz to 960 MHz) covering the UHF RFID system in the world are measured in a $25 \times 15 \times 15\,\text{mm}^3$ microwave chamber, and the measured results are concluded in Figs. 5(b) and (c). The corresponding simulations are also presented here for comparisons. It can be known that the peak radiation gain appears at 915 MHz and drops quickly when offsetting the operating frequency. The radiation gain can keep greater than 2 dBic in the frequency range of 902 MHz to 928 MHz. The quickly dropped radiation gain is mainly due to the narrow operating bandwidth of the inverted-F structure.

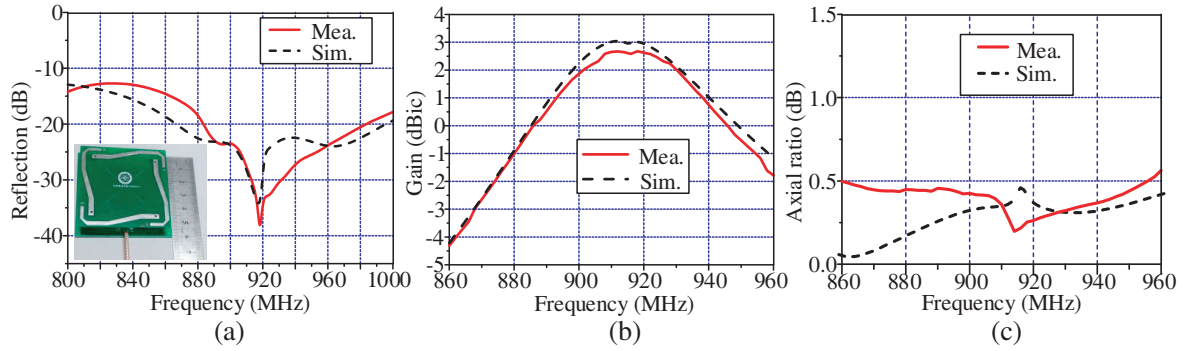

Figure 5. The measured and simulated (a) port reflection, (b) far-field radiation gain, and (c) axial ratio performance for the proposed antenna. The inset of panel (a) is the assembled antenna prototype.

From the measured axial ratio curve as shown in Fig. 5(c), we know that the proposed antenna can achieve a very good circular polarization performance with very low axial ratio, below 0.5 dB in the whole measured frequency band. Fig. 6 shows the measured and simulated radiation patterns at the x-z plane and y-z plane at 915 MHz. It is clearly shown that the proposed antenna possesses quite good radiation performances at both main planes, and the measurements and simulations agree well with each other. The measured half-power beamwidth is larger than 120 deg at both main planes.

Finally, the obtained antenna performances for the proposed structure in this paper are compared to several previously reported UHF RFID hand-held reader antenna realizations. As shown in Table 1, the

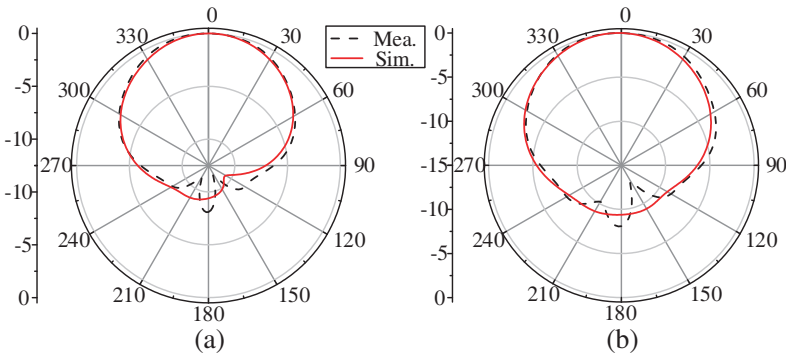

Figure 6. The measured and simulated far-field radiation patterns (normalized) at (a) x-z plane and (b) y-z plane.

Table 1. The comparisons of various UHF RFID handheld reader antennas.

Works	reflection (< -10 dB) (MHz)	axial ratio (< 3 dB) (MHz)	peak gain (dBic)	size (mm^3)
[14]	110	20	1.5	$60 \times 60 \times 1.6$
[16]	90	19	1.4	$60 \times 60 \times 0.508$
[17]	14	13	2.2	$45 \times 45 \times 9$
[18]	28	12	1.0	$60 \times 60 \times 13.4$
[20]	37	8	5.5	$54 \times 54 \times 1.6$
[21]	> 200	> 30	1.5	$60 \times 60 \times 18.7$
[22]	> 200	80	0	$50 \times 50 \times 0.5$
[23]	36	18.6	3.1	$95 \times 100 \times 13.6$
our design	> 200	> 100	2.6	$60 \times 60 \times 10$

hand-held reader antenna realized by the quadrifilar spiral structure [21, 23] has the widest impedance bandwidth and axial ratio bandwidth among all antenna configurations. Moreover, our design has the best axial ratio performance among all the structures. This is mainly due to the well designed and optimized inverted-F structure and the four-way phase shift network. Therefore, the proposed antenna in this paper can be easily used for the universal UHF RFID system.

4. ANTENNA ARRAY SIMULATIONS

In this section, we numerically investigate the performances of an antenna array based on the previously obtained antenna unit. Firstly, a 1×4 array is discussed, and the simulation model is shown in Fig. 7(a). For the antenna array, the distance between adjacent elements is a critical parameter and should be optimized carefully. Theoretically, the distance between adjacent antenna units for achieving maximum gain and minimum mutual coupling is highly related to the gain and beamwidth of such antenna unit. For the obtained antenna unit with wide beamwidth, when the distance d is optimized as 150 mm, the gain can achieve maximum value, and the coupling between antenna elements reaches minimum value. At this stage, the port reflection for each antenna unit can keep unchanged compared to the single antenna condition as shown in Fig. 3(a). When each antenna unit is fed by equal magnitude and phase source, the obtained far-field radiation pattern in y-z plane is shown in Fig. 7(b), and the axial ratio is plotted in Fig. 7(e) (red line). As can be seen, the maximum LHCP radiation gain in the

z-axis is 8.3 dBic, half-power beamwidth 26 deg, and the first side-lobe −13 dB. The axial ratio is below 1.15 dB in the whole frequency band. To control the the direction of the main radiation beam, we can change the phase delay reached to each antenna unit. For example, when the four antenna units are fed with equal magnitude and different phase delays (0, 90, 180, 270 deg for the antenna unit 1 to 4), the obtained radiation pattern in y-z plane is presented in Fig. 7(c). Now the main radiation beam is located at −30 deg with gain of 7.6 dBic and half-power beamwidth of 32 deg. The obtained axial ratio as shown in Fig. 7(e) (green line) also indicates good circular polarization performance. We can further get larger beam deflection and/or inverse beam deflection with larger phase delay and phase advance. On the other hand, the first side-lobe can be further reduced by optimizing the magnitude reached to each antenna. As shown in Fig. 7(d), when the four antenna units are fed with equal phase delay but different magnitudes (1 : 3 : 3 : 1), the obtained radiation pattern in y-z plane has a side-lobe below −22 dB, while the axial ratio is below 1.5 dB as well.

The above discussed 1×4 antenna array can only control the beam direction in the y-z plane. Here we further discuss the 2×2 antenna array to control the beam direction in both y-z plane and x-z plane. The simulation model for the 2×2 antenna array is shown in Fig. 8(a). Also, the distance between adjacent antenna elements is a critical parameter to achieve good radiation pattern, and it is optimized

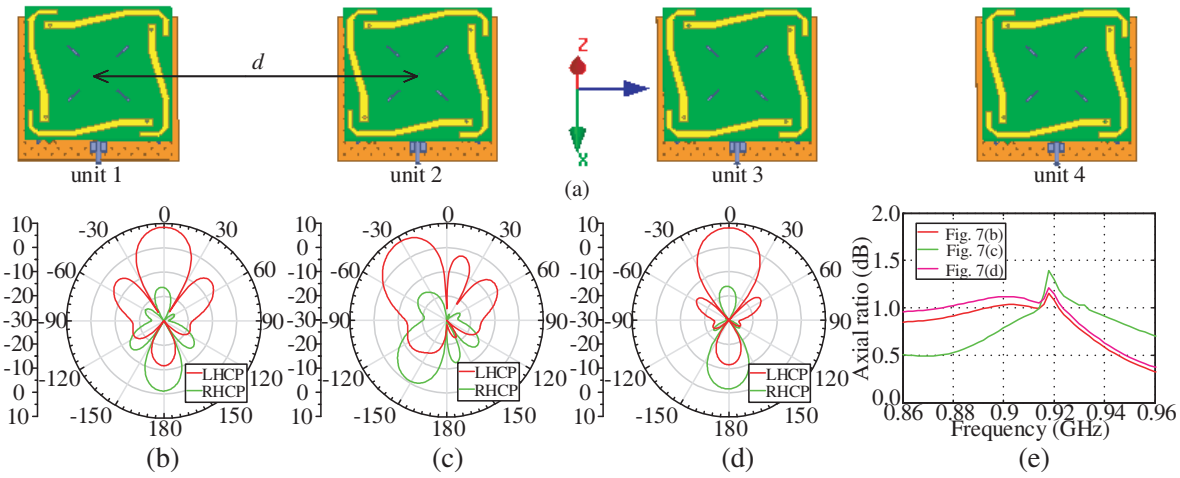

Figure 7. (a) The simulation model for the 1×4 antenna array, and the simulated far-field radiation pattern for (b) equal magnitude and phase delay, (c) equal magnitude and different phase delays, and (d) equal phase delay and different magnitudes. The axial ratio for the previous three conditions are concluded in panel (e).

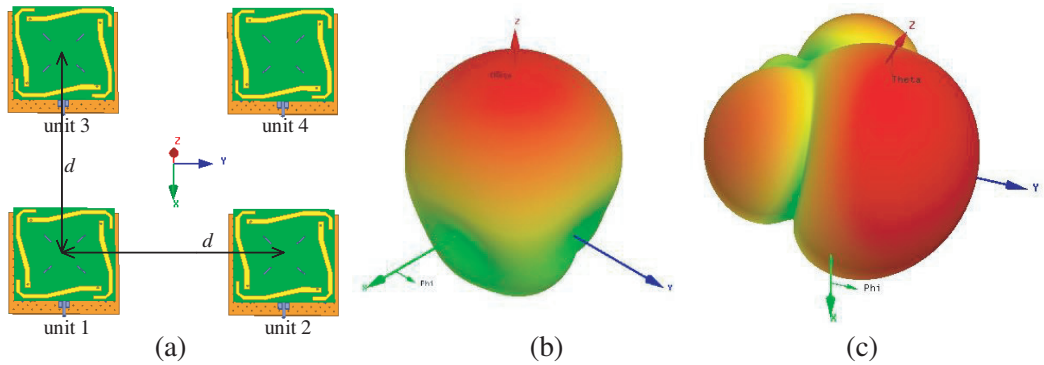

Figure 8. (a) The simulation model for the 2×2 antenna array, and the simulated 3-D far-field radiation pattern for (b) equal magnitude and phase delay and (c) equal magnitude and different phase delays.

as 150 mm as well. When the four antenna units are fed with equal magnitude and phase delay, the simulated 3-D far-field radiation pattern is shown in Fig. 8(b), which indicates that the main beam is located at the exactly z-axis with gain of 8.1 dBic, axial ratio of 0.3 dB, and half-power beamwidth of 57 deg. When the four antenna units are fed with equal magnitude and different phase delays (90, 0, 180, 90 deg for antenna unit 1 to 4), the obtained 3-D far-field radiation pattern is shown in Fig. 8(c), which shows that the main beam is located at the specific direction ($\varphi = 43$ deg and $\theta = 37$ deg) with gain of 7.5 dBic, axial ratio of 1.2 dB, and half-power beamwidth of 70 deg. Therefore, it can be concluded that the antenna array discussed in this section can be used to increase the radiation gain and control the radiation beam direction on a single plane or both planes, for the UHF RFID phase array systems.

5. CONCLUSION

In this paper, we propose and demonstrate a compact circularly polarized antenna experimentaly/numerically based on the resonant quadrifilar spiral structure for the application of UHF RFID handheld reader. The original resonant arms are revised by bending inverted-F structures and printing them on the dielectric substrate to reduce the antenna size and improve the impedance matching performances. The four arms are fed by a four-way phase shift network. The measured results indicate that such an antenna has stable circular polarization performance and wide beamwidth. The frequency band can cover 902 MHz to 928 MHz, which is suitable for most of the popular UHF RFID systems in the world. Moreover, based on the obtained quadrifilar spiral antenna unit, the 1×4 array and 2×2 array are numerically investigated and discussed in details. The array performances, including gain, axial ratio, beam scanning angle and low side-lobe, are discussed by controlling the magnitudes and phase delays. The proposed antenna and array in this paper can be used for most of the UHF RFID systems in the world.

ACKNOWLEDGMENT

This work was supported in part by the National Natural Science Foundation of China (Grant No. 61371047, 61601093), the Guangdong Provincial Science and Technology Planning Program (Industrial High-Tech Field) of China under project contract No. 2016A010101036, and by Sichuan Provincial Science and Technology Planning Program (Technology Supporting Plan) of China under project contracts No. 2016GZ0061.

REFERENCES

1. Finkenzeller, K., *RFID Handbook*, 2nd Edition, John Wiley&Sons, New York, 2003.
2. Karmakar, N. C., *Handbook of Smart Antennas for RFID Systems*, Wiley-IEEE Press, USA, 2010.
3. Chen, X., G. Fu, S. X. Gong, and W. Zhao, "Circularly polarized stacked annular-ring microstrip antenna with integrated feeding network for UHF RFID readers," *IEEE Antennas and Wireless Propagation Letters*, Vol. 9, No. 1, 542–545, 2010.
4. Chen, Z. N., X. Qing, and H. L. Chung, "A universal UHF RFID reader antenna," *IEEE Transactions on Microwave Theory and Techniques*, Vol. 57, No. 5, 1275–1282, 2009.
5. Mireles, E. and S. K. Sharma, "A novel wideband circularly polarized antenna for worldwide UHF band RFID reader applications," *Progress In Electromagnetics Research B*, Vol. 42, 23–44, 2012.
6. Wang, Z., S. Fang, S. Fu, and S. Jia, "Single-fed broadband circularly polarized stacked patch antenna with horizontally meandered strip for universal UHF RFID applications," *IEEE Transactions on Microwave Theory and Techniques*, Vol. 59, 1066–1073, 2011.
7. Yusuf, Y. and X. Gong, "A low-cost patch antenna phased array with analog beam steering using mutual coupling and reactive loading," *IEEE Antennas and Wireless Propagation Letters*, Vol. 7, No. 1, 81–84, 2008.
8. Abbak, M. and I. Tekin, "RFID coverage extension using microstrip-patch antenna array," *IEEE Antennas and Propagation Magazine*, Vol. 51, No. 1, 185–191, 2009.

9. Liao, W.-J., S.-H. Chang, Y.-C. Chu, and W.-S. Jhong, "A beam scanning phased array for UHF RFID readers with circularly polarized patches," *Journal of Electromagnetic Waves and Applications*, Vol. 24, Nos. 17–18, 2383–2395, 2010.
10. Nasimuddin, Z. N. Chen, and X. Qing, "Asymmetric-circular shaped slotted microstrip antennas for circular polarization and RFID applications," *IEEE Transactions on Antennas and Propagation*, Vol. 58, No. 12, 3821–3828, 2010.
11. Nasimuddin, Z. N. Chen, and X. Qing, "A compact circularly polarized cross-shaped slotted microstrip antenna," *IEEE Transactions on Antennas and Propagation*, Vol. 60, No. 3, 1584–1588, 2012.
12. Agarwal, K., Nasimuddin, and A. Alphones, "RIS-based compact circularly polarized microstrip antennas," *IEEE Transactions on Antennas and Propagation*, Vol. 61, No. 2, 547–554, 2013.
13. Nasimuddin, X. Qing, and Z. N. Chen, "A wideband circularly polarized stacked slotted microstrip patch antenna," *IEEE Antennas and Propagation Magazine*, Vol. 55, No. 6, 84–99, 2013.
14. Lin, Y. F., Y. K. Wang, H. M. Chen, and Z. Z. Yang, "Circularly polarized crossed dipole antenna with phase delay lines for RFID handheld reader," *IEEE Transactions on Antennas and Propagation*, Vol. 60, No. 3, 1221–1227, 2012.
15. Lee, J.-N. and J.-H. Jung, "Design of the planar cross dipole reader antenna for UHF RFID systems," *Journal of Electromagnetic Waves and Applications*, Vol. 26, No. 7, 962–972, 2012.
16. Ta, S. X., H. Choo, and I. Park, "Planar, lightweight, circularly polarized crossed dipole antenna for handheld UHF RFID reader," *Microwave and Optical Technology Letters*, Vol. 55, No. 8, 1874–1878, 2013.
17. Bang, J.-H., C. Bat-Ochir, H.-S. Koh, E.-J. Cha, and B.-C. Ahn, "A small and lightweight antenna for handheld RFID reader applications," *IEEE Antennas and Wireless Propagation Letters*, Vol. 11, 1076–1079, 2012.
18. Lin, Y.-F., C.-H. Lee, S.-C. Pan, and H.-M. Chen, "Proximity-fed circularly polarized slotted patch antenna for RFID handheld reader," *IEEE Transactions on Antennas and Propagation*, Vol. 61, No. 10, 5283–5286, 2013.
19. Hsu, H.-T. and T.-J. Huang, "A 1×2 dual-band antenna array for radio-frequency identification (RFID) handheld reader applications," *IEEE Transactions on Antennas and Propagation*, Vol. 62, No. 10, 5260–5267, 2014.
20. Farswan, A., A. K. Gautam, B. K. Kanaujia, and K. Rambabu, "Design of koch fractal circularly polarized antenna for handheld UHF RFID reader applications," *IEEE Transactions on Antennas and Propagation*, Vol. 64, No. 2, 771–775, 2016.
21. Son, W. I., W. G. Lim, M. Q. Lee, S. B. Min, and J. W. Yu, "Printed square quadrifilar spiral antenna for UHF RFID reader," *IEEE AP-S International Symposium*, 303–308, 2007.
22. Lee, S.-J., D.-J. Lee, H.-S. Jang, H.-S. Tae, and J.-W. Yu, "Planar square quadrifilar spiral antenna for mobile RFID reader," *The 9th European Radar Conference (EuRAD)*, 618–621, 2012.
23. Liu, Q., J. Shen, H. Liu, Y. Wu, M. Su, and Y. Liu, "Low-cost compact circularly polarized directional antenna for universal UHF RFID handheld reader applications," *IEEE Antennas and Wireless Propagation Letters*, Vol. 14, 1326–1329, 2015.
24. Kilgus, C. C., "Multielement, fractional turn helices," *IEEE Transactions on Antennas and Propagation*, Vol. 16, No. 4, 499–500, 1968.